Available online at www.sciencedirect.com

ScienceDirect

Journal of Ocean Engineering and Science 1 (2016) 256–267

www.elsevier.com/locate/joes

Original Article

Reactive power control and optimisation of hybrid off shore tidal turbine with system uncertainties

Asit Mohanty[a,*], Meera Viswavandya[b], Prakash K Ray[c], Sthitapragyan Mohanty[d]

[a] *Department of Electrical Engineering, College of Engineering and Technology, Bhubaneswar 751003, India*
[b] *Associate Professor, CET Bhubaneswar, India*
[c] *Department of Electrical Engineering, IIIT, Bhubaneswar 751003, India*
[d] *Research Scholar, CET Bhubaneswar, India*

Received 10 March 2016; accepted 24 June 2016
Available online 9 July 2016

Abstract

This paper projects an isolated hybrid model of Offshore wind-diesel-tidal turbine and discusses the stability and reactive power management issue of the whole system. The hybrid system often loses its stability as it becomes prone to uncertain load and input parameters and therefore the necessity of Reactive power management becomes necessary. The overall stability of the hybrid offshore wind-diesel-tidal turbine is made possible by the management of reactive power in the hybrid system through the application of FACTS devices. And therefore the dynamic hybrid model of the DFIG and DDPMSG based offshore wind-diesel-tidal turbine is analysed for stability with different input parameters like wind and tidal energies. For detailed modelling and simulation, a small signal model of the whole hybrid system is designed and reactive power management of the system is achieved by the incorporation of a STATCOM controller. For improvement of stability and reactive power compensation of the hybrid system, GA and PSO optimised STATCOM controller is used.

Keywords: Offshore wind-diesel-tidal hybrid system; DFIG; DDPMSG; Reactive power; STATCOM; PSO.

1. Introduction

Remote places situated far away from the main grid always remain devoid of power. Therefore it is always a challenge for the power engineers to supply adequate power to the loads situated far away. Renewable energy sources play a vital role in providing power to these localities as power can be generated near the loads in these localities. Multiple renewable energy sources are often utilised as hybrid systems in these places to boost the generating capacity and to face the uncertainty nature of renewables. Hybrid systems like wind-pv,wind-fuel cell, wind-diesel, wind-bio mass are quite common combination and are often utilised in standalone mode. In recent days wind offshore power plants are operating in different corners of the world are found a good number of research articles are published about this technology. But in contrary the tidal energy conversion is a technology that is still in development. Combination of these two vital energy sources is a great benefit to the mankind particularly for the remote islands and all the offshore places. This hybrid energy source acts in a combined manner and produce energy for the isolated loads. The offshore wind tidal combined system can be of great benefit to the remote islands where the extension of electricity grid is a costly affair.

The combination of offshore and tidal turbines offer combined continuous power as it is a well-known fact that the renewable energies source as individual they do not produce energy continuously eradicate the intermittent power supply of the individual sources [1–5]. The isolated hybrid system uses a diesel engine which works as a backup for the combined system. During the hybrid operation the two energy sources compensate one another in order to produce energy in continuous period. Generally the wind turbine uses an in-

* Corresponding author.
E-mail address: asithimansu@gmail.com (A. Mohanty).

http://dx.doi.org/10.1016/j.joes.2016.06.005

Nomenclature

$P, Q_{DFIG/DDPMG}$	Real power Reactive power (DFIG/DDPMG)
P_{SG} Q_{SG}	Real Power, Reactive Power- (SG)
E_M, ΔE_M	Electromagnetic energy and small change of Energy. (DFIG)
$\Delta Q_{STATCOM}$	Reactive generated by STATCOM
ΔQ_{COM}	Reactive Power (Compensator)
K_A, K_E, K_F	Gain Constants of Voltage Regulator, Exciter, Stabilizer
ΔV	Incremental Change in terminal Voltage
K_α, K_v	Exciter Gain, Gain Energy loop
$T\alpha$, T_r, T_s	Exciter, rising, settling time const.
X_d X'_d	Direct axis reactance of SG under steady state and transient
$\Delta\alpha$	Phase angle -Compensators
ΔE_q	Incremental Change in Internal Armature Voltage
ΔE_{fd}	Change in the Voltage of the Exciter
η	Performance Index

duction generator as it is robust in nature. In present days DFIGs are frequently used as wind turbines [6–9]. The tidal turbine functions just like the wind turbine and uses DFIG and DDPMSG. The tidal turbine is the most predictable energy source and gives continuous power supply. The offshore wind turbine also gets continuous wind supply in comparison to wind turbine in the mainland [10–15]. The combination with the diesel backup becomes a reliable energy source for remote locations. The wind-tidal isolated hybrid systems are reliable and need low maintenance. Inorder to achieve optimum result there is always a need of correct size of each component of the−energy system and optimisation of energy management within the system. As the wind remains much more constant in the sea than the land, the sea proves to be advantageous for wind turbines. The tidal turbine has lot of similarities with wind turbines as far as the electrical side layout and modelling are concerned. It is also true that the speed of water currents is lower than the wind speed but the water density is more than the air density. The wind turbines function at a higher rotational speeds and lower torque than tidal in-stream turbines as the water density is higher than the air density. As tidal turbines are much more predictable they are integrated with electrical power grid in a easier way [16,17]. Areas with limited grid capacity always pose challenges before the power engineers Day by day the penetration of tidal current energy is increasing into the electrical grid system and more and more number of tidal based hybrid systems are coming to the picture. But the stability of these tidal based hybrid systems are always a challenge for the researchers. A tidal turbine generator responses to network voltage and frequency and with that it maintains electrical performance requirements such as reactive power capability and system voltage profile [18–20].

2. Modelling of offshore wind-tidal hybrid power system

In a simplified view the hybrid system as shown in Fig. 1 composes an offshore wind turbine and a tidal turbine with power electronics based FACTS devices for reactive power compensation and enhanced power quality. The FACTS devices also help in solving the grid connection problem and storage difficulties. The hybrid system not only provides combined power to the existing loads but enhances the overall reliability of the system. The diesel generator is usually used in all the hybrid systems as back up for power production. The tidal turbine becomes comparatively predictable and reliable because of its continuous power supply capability

$$\Delta P_{hybrid} = \Delta P_{wind} + \Delta P_{tidal} \tag{1}$$

$$\Delta Q_{DDPMSG} + \Delta Q_{DFIG} = \Delta Q_{SG} + \Delta Q_{COM} \tag{2}$$

When connected to the load the reactive power balance equation becomes as in Fig. 2

$$\Delta Q_{DDPMSG} + \Delta Q_{DFIG} + \Delta Q_L = \Delta Q_{SG} + \Delta Q_{COM} \tag{3}$$

The system terminal voltage is highly affected by the reactive power balance equation and it can be summerised as

$$\Delta V(s) = \Delta Q_{SG}(s) + \Delta Q_{COM}(s) - \Delta Q_{DDPMSG}(s) - \Delta Q_{DFIG}(s) - \Delta Q_L(s) \tag{4}$$

2.1. Modelling of offshore-wind turbine and tidal turbine (DFIG)

DFIG is a wound rotor asynchronous generator where power flows between the rotor and grid through AC/DC/AC converters. Single line diagram of DFIG is shown in Fig. 3 where the supply side converter keeps the DC link voltage constant without considering the direction of rotor power flow.

Depending on the stator flux vector position the induction machine is controlled in synchronous rotating dq axis frame. The active and reactive power control has been realised by controlling Iqr and Idr through the rotor side converter. The diesel engine as a conventional DG unit manages active and reactive power in high load demand. Reactive power control of the output is done by separate PI controllers and the outer loop compares the voltage of generator DFIG with that of reference voltage.

$$Q_{DFIG} = \frac{L_m}{L_{ss}} V_1 I_{dr} - \frac{V_1^2}{w_s L_{ss}} \tag{5}$$

The linearised form of the reactive power of proposed DFIG can be calculated as

$$_{DFIG}(s) = K_f \Delta I_{dr}(s) + K_e \Delta V(s) \tag{6}$$

where $K_f = \frac{L_m V_1}{L_{ss}}$ and $K_e = \frac{L_m I_{dr}}{L_{ss}} - \frac{2V_1}{w_s L_{ss}}$

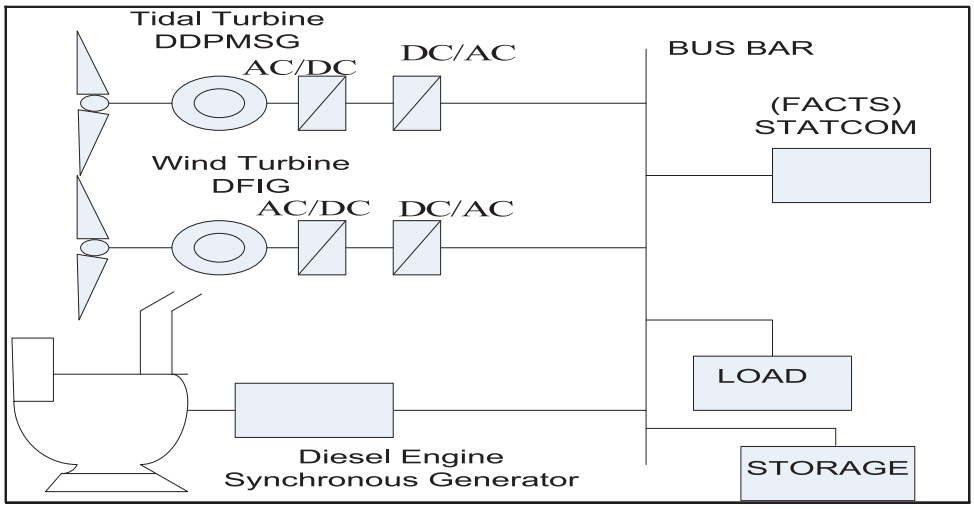

Fig. 1. Offshore wind-diesel-tidal hybrid system.

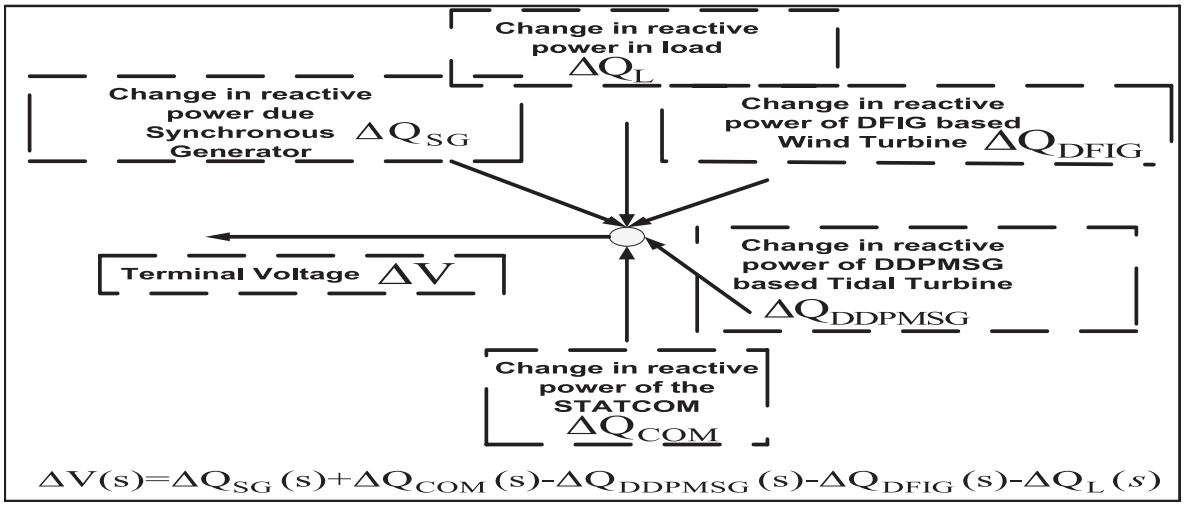

Fig. 2. Reactive power exchange between different components of offshore hybrid system.

Rotor d axis reference current, the output signal of the voltage loop PI controller are

$$\Delta I_{dr}^{ref} = \left(K_P + \frac{K_I}{s}\right)\left[\Delta V^{ref}(s) - \Delta V(s)\right] \tag{7}$$

An over damped second order system is designed according to a first order system with equal settling time. Dynamic inner loop is modelled and is equal to

$$\Delta I_{dr} = \frac{1}{(1+\frac{t_s}{4}s)\Delta I_{dr}^{ref}} \tag{8}$$

$$\underline{x} = \left[\Delta I_{dr}^{ref}, \Delta I_{dr}, \Delta V, \Delta E_{fd}, \Delta V_a, \Delta V_f, \Delta E'_q\right]^T$$
$$\underline{u} = [\Delta V_{ref}]$$
$$\underline{w} = [\Delta Q_L] \tag{9}$$

The state space model of the offshore wind-diesel-tidal hybrid system can be modelled as shown in Fig. 4

$$\dot{x} = Ax + Bu + Cw$$

Where x,u,w are state, control and disturbance vectors of the wind-diesel-tidal hybrid system and A,B,C are the matrices of appropriate dimensions.

2.2. Modelling of offshore wind-tidal turbine (DDPMSG)

In case of a direct drive PMSG turbine (DDPMSG), the generator-side converter is a diode rectifier and the grid side converter is a Pulse Width Modulation (PWM) inverter as shown in Figs. 5 and 6. These are utilised to meet the dc bus voltage and regulate the grid-side power factor that is controlled independently through the decoupled d-q vector control approach. The DC link decouples the operation of the two converters and the PMSG speed changes during voltage dips are negligible that is because the power supply to the DC circuit from the machine-side converter is approximately constant.

DDPMSG is nothing but a synchronous generator with constant rotor flux linkage. The equivalent circuit is shown

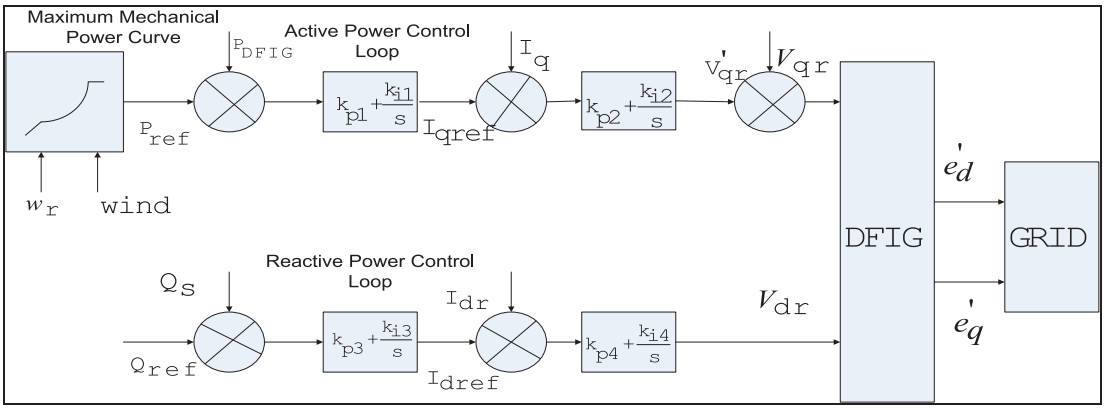

Fig. 3. Simplified DFIG single line diagram.

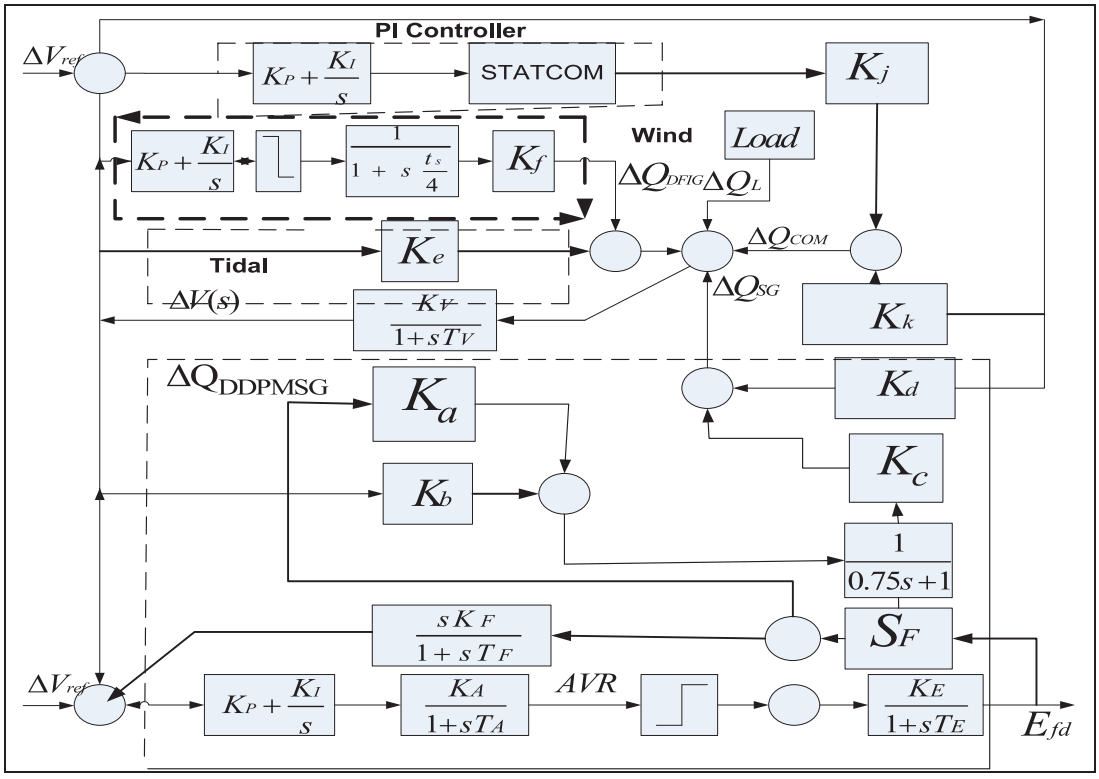

Fig. 4. Transfer function of DFIG/DDPMSG based wind-diesel-tidal hybrid system.

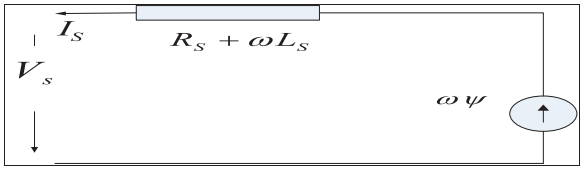

Fig. 5. Equivalent circuit of DDPMSG.

and the standard equation is given as

$$L_S \frac{di_{ds}}{dt} = -v_{ds} - R_s i_{ds} + L_s w i_{qs} \quad (10)$$

$$L_S \frac{di_{qs}}{dt} = -v_{qs} - R_s i_{qs} - L_s \omega i_{ds} + \omega\psi \quad (11)$$

*v*ds and *v*qs are direct (d) and quadrature (q) axis stator voltages and ids and iqs are the d and q axis stator currents. R_S is resistance of the stator and Ls is inductance of the stator,ω is generator electrical speed

The Power equations are

$$P_S = V_{ds} i_{ds} + V_{qs} i_{qs} \quad \text{and} \quad Q_S = V_{qs} i_{ds} - V_{ds} i_{qs}$$

The generator side converter not only controls the output active power of the generator but minimises the power losses of the generator. The active power is controlled via *v*qs and

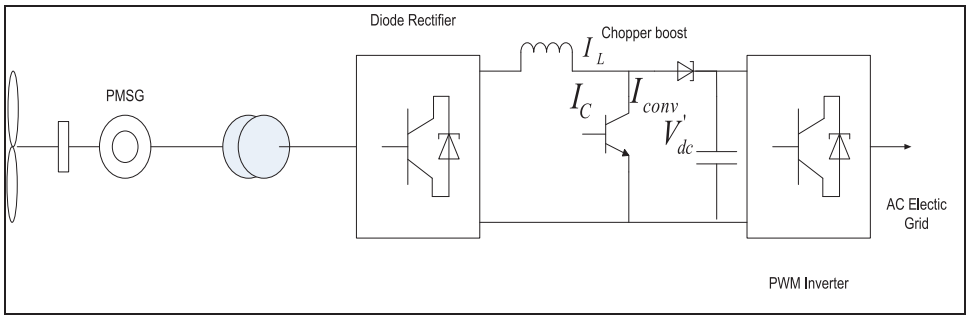

Fig. 6. Configuration of a DDMSG Generator.

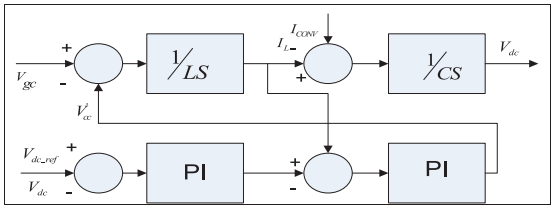

Fig. 7. Control loop for the DC-Link voltage.

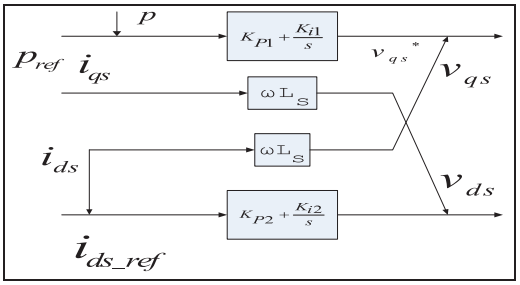

Fig. 8. Generator side converter control block diagram.

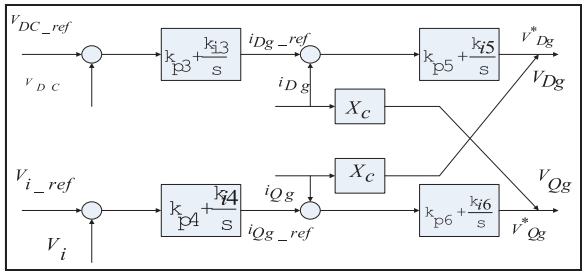

Fig. 9. Grid side converter block diagram.

the power losses of the generator are lessened by controlling *ids* to zero. The control is implemented with *v*ds. The control block diagrams are shown. The control equations are given by

$$\dot{x} = f(x, z, u) \tag{12}$$

$$z = g(x, u) \tag{13}$$

$$x = \left[\omega_r, i_{ds}, i_{qs}, v_{DC}, x_1, x_2, x_3, x_4, x_5, x_6\right]^T \tag{14}$$

$$z = \left[v_{ds}, v_{qs}, v_{Dg}, v_{Qg}\right]^T \tag{15}$$

$$u = \left[v_{Dl}, v_{Ql}, i_{Dg}, i_{Qg}\right]^T \tag{16}$$

x,z,u are the vectors associated with the state variables.

By linearising Eqs. (17) and (18) we get a relationship like

$$\Delta\dot{x} = A\Delta'_x + B'_z + C'_u\,\Delta z = D'_x + E'_u$$

The grid side converter control maintains the DC –link voltage and the terminal voltage constant. It helps the system in controlling the reactive power and enhancement of voltage stability. The DC-link voltage and the terminal voltage of the tidal turbine are controlled by V_{Dg} and V_{Qg}.

$$V_{Dg} = K_{P5}(-K_{P3}\Delta V_{DC} + K_{i3}x_3 - iD_g)K_{i5}x_5 + X_c i_{Qg} \tag{17}$$

$$V_{Qg} = K_{P5}(-K_{P4}\Delta V_t + K_{i4}x_5 - iQ_g)K_{i5}x_6 + X_c i_{Dg} \tag{18}$$

K_{P5}, K_{i5} are gains of grid side converter. K_{P4}, K_{i4} are gains of terminal voltage regulator K_{P3} and K_{i3} are the gains of DC bus voltage regulator (Figs. 7–9).

Where A is the combined system state matrix of DDPMSG based tidal energy conversion system.

$$\underline{x} = \left[\Delta\omega_t, \Delta i_{ds}, \Delta i_{qs}, \Delta V_{dc}, \Delta V, \Delta E_{fd}, \Delta V_a, \Delta V_f, \Delta E'_q\right]^T$$
$$\underline{u} = [\Delta V_{ref}]$$
$$\underline{w} = [\Delta Q_L]$$

Wind-diesel-tidal hybrid system with DDPMSG integrated into the power grid can be modelled as

$$H\frac{dw_t}{dt} = T_M - T_e$$
$$T_M = \frac{0.5\rho\pi R^2 C_p V_w^3}{\omega_t} \text{ where}$$
$$C_p = \frac{1}{2}\left(\frac{RC_f}{\lambda} - 0.022\beta - 2\right)e^{-0.255(RC_f/\lambda)}$$
$$T_e = -p\psi i_{qs}$$

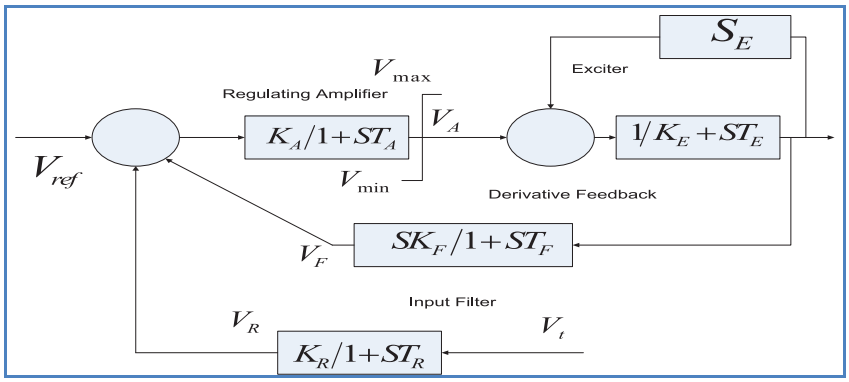

Fig. 10. IEEE Type 1 AVR Model.

2.3. AVR system modelling

Synchronous generator is preferred with DG set. This is used as primary source of electric supply and an alternative to the grid power. SG caters to reactive power need of the system and controls the reactive power need of the offshore wind-diesel-tidal hybrid system. The SG must be controlled in a careful manner so as to prevent the rotor speed accelerating through synchronous speed.

The synchronous generator equation is given by

$$Q_{SG} = \frac{(E'_q V\cos\delta - V^2)}{X'_d} \text{ (Transient)} \tag{19}$$

For small change the equation is

$$\Delta Q_{SG} = \frac{V\cos\delta}{X'd\Delta E'q} + \frac{E'q\cos\delta - 2V}{X'd\Delta V} \tag{20}$$

$$\Delta Q_{SG}(S) = K_a \Delta E'q(S) + K_b \Delta V(S)$$
$$K_a = \frac{V\cos\delta}{X'd} \text{ and } K_b = \frac{E'q\cos\delta - 2V}{X'd} \tag{21}$$

Excitation system not only provides direct current to the synchronous machine field winding but performs control and protective functions in a hybrid power system by controlling the field voltage and current.

The excitation system is represented by a single time constant automatic high gain AVR System. IEEE type-I AVR system used in this modelling is shown in Fig. 10.

2.4. Modelling of STATCOM controller

Basically a STATCOM is a solid state synchronous voltage source which is equivalent to an ideal synchronous machine that produces a set of three sinusoidal voltages at a fundamental frequency. The configuration of STATCOM is made of voltage source converter with a coupling transformer and dc capacitor. The control of the reactive current is achieved by the variation of δ(phase angle) and α(angle of fundamental output voltage). The configuration of STATCOM is shown in Fig. 11.

The reactive power injected by STATCOM is

$$Q + V^2B - KV_{dc}VB\cos(\delta - \alpha) + KV_{dc}VG\sin(\delta - \alpha) = 0 \tag{22}$$

with incremental change

$$\Delta Q_{STATCOM}(S) = K_J \Delta\alpha(S) + K_K \Delta V(S) \tag{23}$$

$$K_k = KV_{dc}B_{sin\alpha} \text{ and } K_L = KV_{dc}B_{cos\alpha} \tag{24}$$

3.1. Design of STATCOM controller

For industry generally proportional integral type of controllers are used. The effectiveness of PI controller based STATCOM can be enhanced by tuning the proportionality constants like Kp and Ki. The tuning process is further enhanced by the optimisation process through GA and PSO etc. The controllers for STATCOM and DC voltage regulator are better tuned by optimising by GA and PSO. In both the cases of GA and PSO the objective function has been determined as the integral time absolute error (ITAE). This index has been used to optimise and control tuning. The GA and PSO optimisations minimise the performance index ITAE. The population size, number of chromosomes; mutation rate and mating rate have been considered as 24, 4, 10% and 50%, respectively for achieving better results. Finally the optimum results are calculated by minimising the performance index.

3.2. Objective function

Objective function determines the mathematical relationship between the optimised parameters. Here in this problem GA and PSO are used to optimise the objective function. Optimisation of objective function damps out the oscillations of STATCOM controller. The process is done by maximisation of damping ratio of poorly damped eigen values of STATCOM controller. Also in this process the stability margin of the hybrid system gets enhanced and thereby better damping with minimum increment in terminal voltage is found out. The optimisation of performance index also enhance the stability margin of the hybrid system by reducing the overshoot

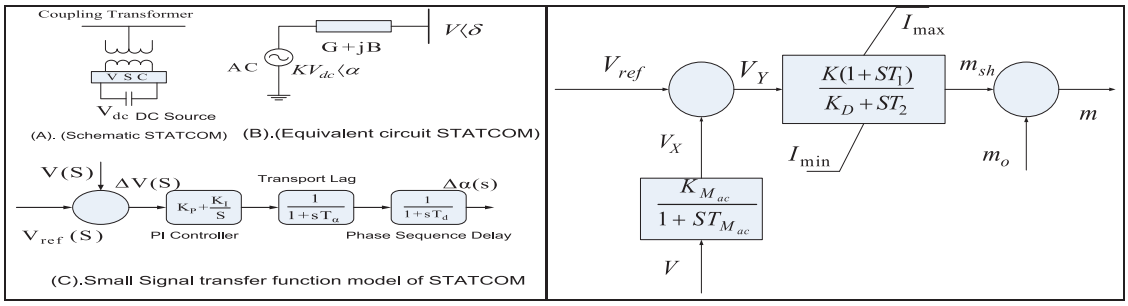

Fig. 11. STATCOM with PWM Voltage control.

Table 1
Optimal Parameters.

Type of System Controller	Kp	Ki	IAE	ITSE	ITAE	Rise Time	Overshoot
STATCOM based PI Controller	65	13,500	961.2	24.4	15.92	0.0943	0.0198
STATCOM based system(GA)	35	6000	897.7	23.3	11.45	0.0345	0.0180
STATCOM based system(PSO)	31	5100	607.8	10.67	8.19	0.355	0.0126

(Mp), settling time (ts), rising time (tr) and steady state error (Ess) of the terminal voltage. Indices like Inegral absolute error (IAE), Integral square error (ISE) and Integral square time error (ISTE) are considered for calculation of the performance index. Proportional–integral (PI) type controllers are usually utilised in industrial applications and it is quite effective in its performance The PI type controllers are tuned with genetic algorithms (GA) and PSO optimisation method and in both the GA and PSO optimisation, the objective function has been determined as the integral time absolute error (ITAE) as mentioned in Table 1.

$$IAE = \int_0^\infty |V_t(t)|dt$$

$$ISE = \int_0^\infty V_t^2(t)dt$$

$$ISTE = \int_0^\infty tV_t^2(t)dt$$

3.3. PSO based STATCOM controller

Particle swarm optimisation takes inspiration from the social behaviour of bird flocking and it is an evolutionary algorithm. It was first proposed by Kennedy and Eberhaut in 1995 and further elaborated in 1997. The actual concept is how birds are able to prey for food in a confined area. Every bird is taken as a particle and therefore this evolutionary algorithm is named by particle swarm optimisation. It is very useful to find the optimised solution with fewer parameters and it converges the optimised solution quickly. It is also very easy to implement because of its high efficiency and effectiveness. PSO is quite popular for optimisation of the values of PI controller and therefore this algorithm is used frequently to optimise the value of Proportional and integral constants of PI Controller. In PSO each particle changes its present position to a new position with respect to the new velocity, distance to pbest, previous positions and the distance to gbest in that particular problem. After that particle's velocity with its new position are updated as per Fig. 12.

$$V_i^d(t+1) = W(t)V_i^d(t) + C_1Xr_1X(pbest_i^d - X_i^d(t)) + C_2Xr_2X(gbest_i^d - x_i^d(t))$$
$$gbest_i^d = x_i^d(t+1) + V_i^d(t+1) \quad (25)$$

$$W(t) = rand\ X\ \frac{t}{t_{max}}X(W_{max} - W_{min}) + W_{min} \quad (26)$$

$V_i^d(t)$ is the ith particle in the dth dimension at iteration t and $X_i^d(t)$ is the current position of the particle.

$C1$ and $C2$ are the acceleration coefficients. $r1$ and $r2$ represent random numbers between [0, 1]

A typical PSO algorithm can be summarised as shown in Fig. 12.

First step: Define of number of particles, and initialise their initial speeds and positions.

Second step: Evaluation of the fitness of each particle.

Third step: For each particle, compare the above calculated fitness with its present best fitness. If the former is better, then update its present best fitness by the former, and update its best position by present position.

Forth step: For each particle, compare its fitness with the swarm's global best fitness. If the former is better, then update global best fitness by the former, and update global best position by the being compared particle's best position.

Fifth step: Update each particle's position and speed according to the Eqs. (13)–(15).

Sixth step: Repeat from step 2 until termination conditions are fulfilled.

In this paper, the PSO is used to determine the optimum PI controller parameters.

4. Simulation results and discussion

The offshore wind-diesel-tidal hybrid system is system with varying load inputs and disturbances and observed un-

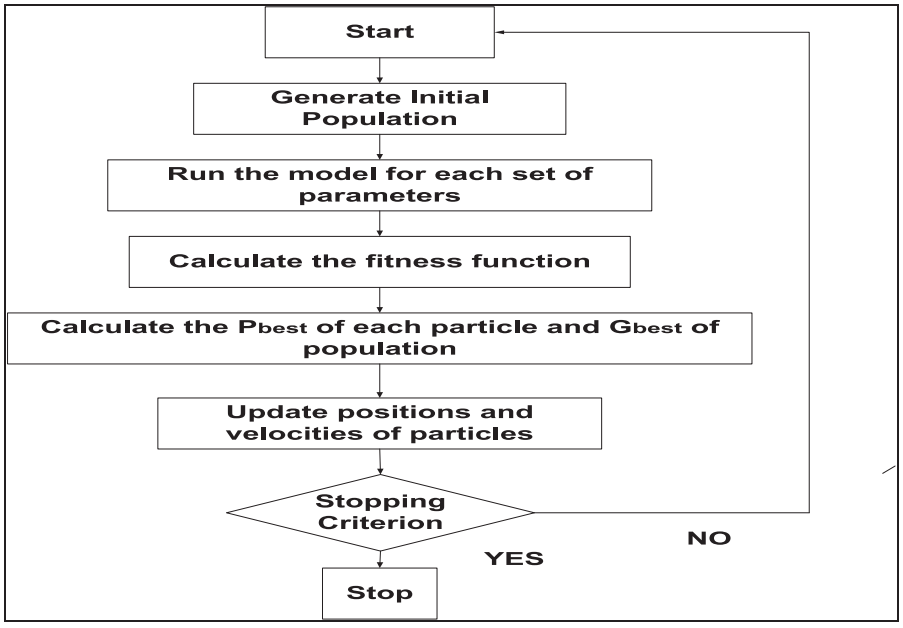

Fig. 12. Flow chart of controller with PSO optimisation.

Table 2
Maximum Deviation Of different system Parameter.

System Parameters	DFIG offshore wind	Maximum Deviation DDPMSG offshore wind	With STATCOM
DelV	0.07	0.067	0.062
Del Alpha	2.6	1.5	8
Del QSG	0.5	0.49	0.485
Del Eq	0.06	0.058	0.056

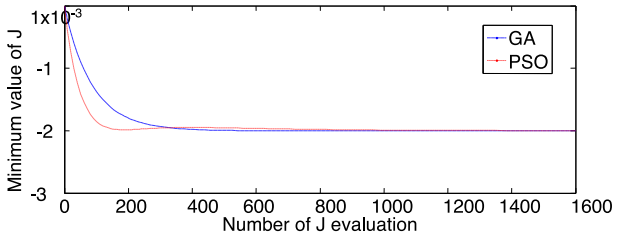

Fig. 13. Convergence Curve for GA and PSO algorithm.

der various operating conditions. During simulation the performance of different controllers are analysed and their contribution in minimisation of voltage deviation in the hybrid system has been discussed. The system performance under normal loading and uncertain load variation (±5%) is examined to know the load sharing, controller performance and the deviation of system voltage profile. Also the hybrid system performance is watched with fixed and variable inputs like wind and tide. Detailed analysis with and without controller have been carried out and improvements have been noticed with GA and PSO based optimised STATCOM Controller as shown in Fig. 13, Fig. 14(a-d), Fig. 15(a-c) and Table 2.

4.1. Stability analysis

4.1.1. Eigen value & participation factor analysis

The Eigen values are set of scalars and are associated with a linear system of equations. which are sometimes generally known as characteristic roots or characteristic values. Determination of the eigenvalues and eigenvectors of a system is Very important in engineering which is equivalent to matrix diagonalisation. It has common applications as stability analysis, each and every eigenvalue is paired with a corresponding eigenvector $(A - \lambda I)X = 0$. Where I is called the identity matrix. As discussed in Cramer's rule, a linear system of equations has nontrivial solutions if and only if the determinant vanishes. The solutions of equation $\det(A - \lambda I) = 0$. This equation is known as the characteristic equation of A and the left-hand side is known as the polynomial. The eigen values of DFIG and DDPMSG based hybrid systems are mentioned in Table 3.

The Participation matrix of the hybrid system indicates a relationship between the selected state variables and the eigen values which combines both right and left Eigen vectors. It clearly shows the association between state variables and Eigen values as shown in Table 4.

$$[P] = [p1.....pn] \tag{24'}$$

$$pi = [pki] = [fki\varphi ik] \tag{25'}$$

Where ϕki= the element of the kth row and ith column of the matrix [ϕ]. The stability of wind-diesel-tidal hybrid power system depends on the eigen values under different loading condition and input power. It is in case of DDPMSG the eigen values lie more to the left hand side of s plane in comparison

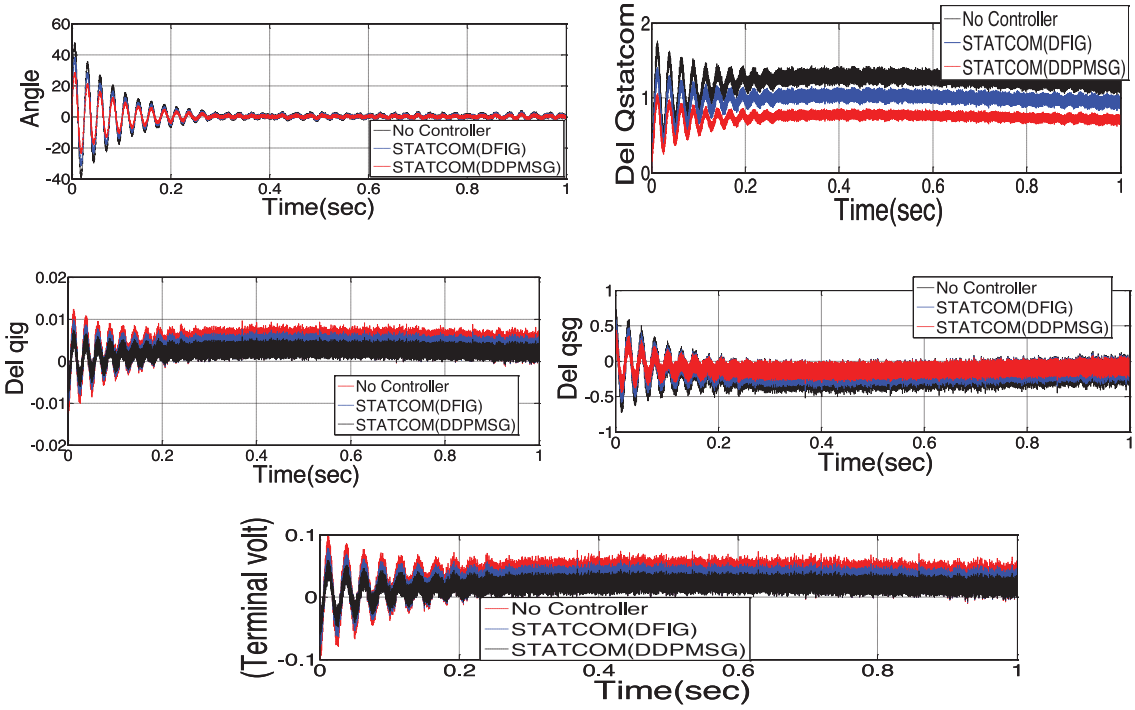

Fig. 14. (a–d)-Comparison of performances of different parameters with DFIG and DDPMSG based offshore wind-diesel-tidal hybrid system.

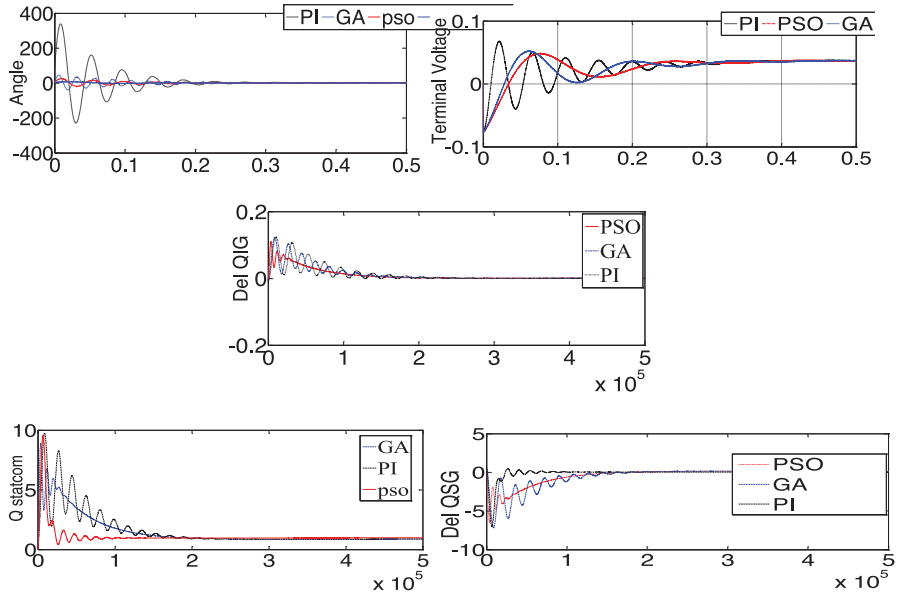

Fig. 15. (a–c)- Comparison between controllers based on GA and PSO.

to DFIG and thereby indicating enhancement of damping and stability.

Further the stability analysis of the hybrid wind-diesel-tidal hybrid system has been processed with DFIG and DDPMSG based turbines and the performances have been compared based on Bode, Nyquist circle criterion as shown in Fig. 16(a–f). The Bode plots stand for the frequency plots of the magnitude and phase of the open-loop frequency transfer function where magnitude has been plotted in dB (decibels) and the phase angle in degrees.

These plots Fig. 16(a,b), represent the static gains and dynamic roots by providing informations regarding the phase and gain margins. It indicates the closed-loop frequency response parameters and are extremely helpful in assessing the transient stability of the offshore hybrid system. Fig. 16(c) shows the pole zero and Nichols chart of the offshore hybrid system and analyse the stability criteria. In Nyquist stability criterion, a system attends stable stage if the value of feedback gain k is such that the point -1/K will never lie on the right half of stability plane G (s), which is the transfer function of

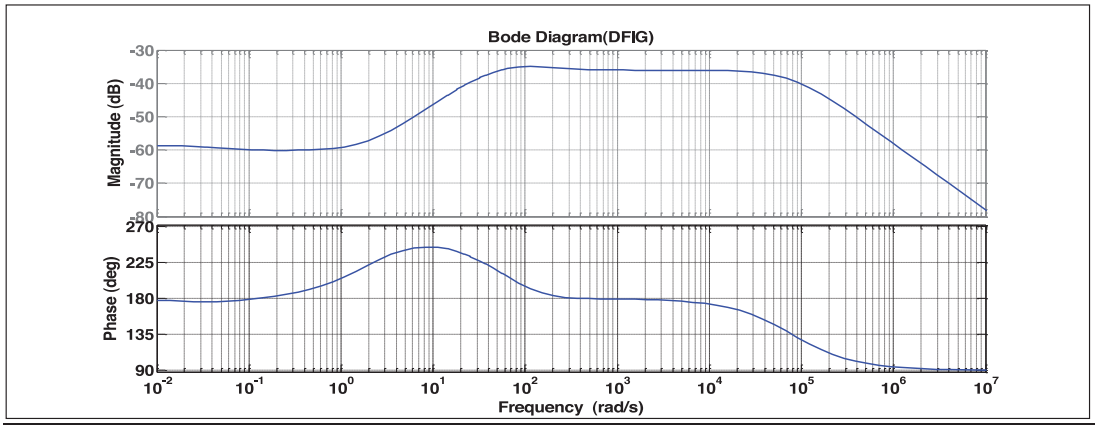

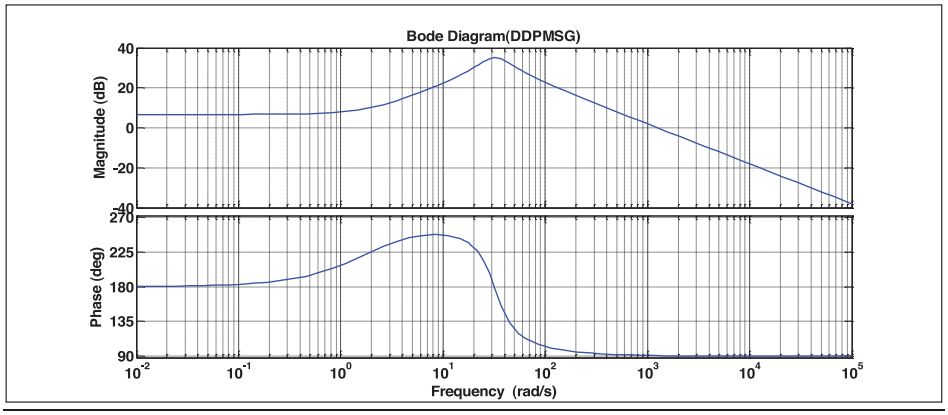

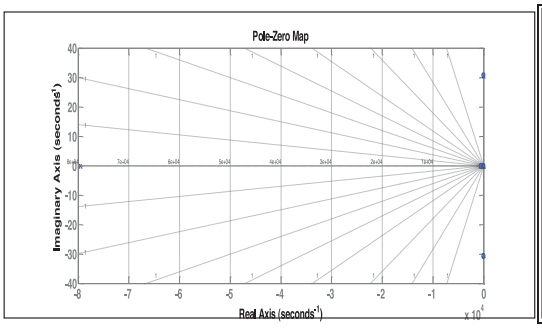

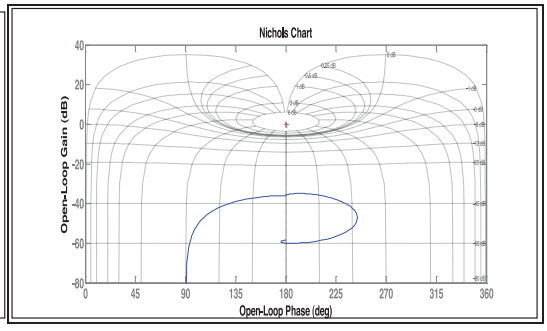

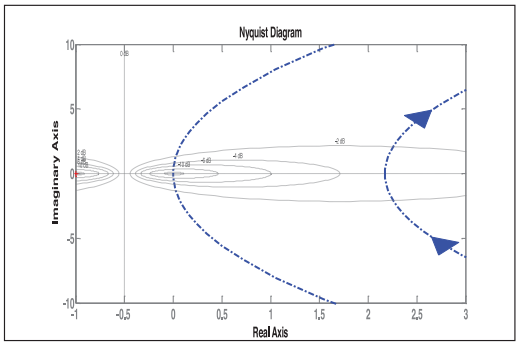

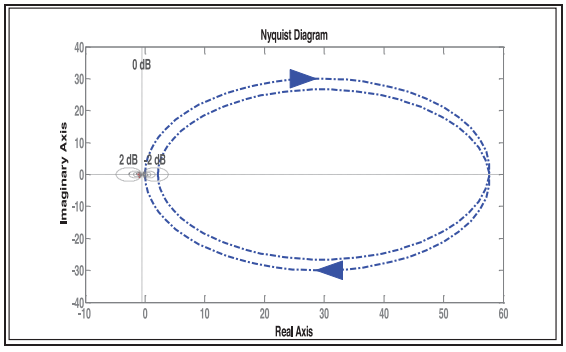

Fig. 16. (a–f)-Stability analysis of the hybrid system through Bode,Nyquist,Pole zero and Nichols chart.

Table 3
Comparison of Eigen values and Damping Ratio of DFIG and DDPMSG.

DFIG based Wind- Diesel-Tidal Turbine			DDPMSG based Wind- Diesel-Tidal Turbine		
Eigen value	Damping	Frequency	Eigen value	Damping	Frequency
−3.83e−2	1.00e+00	3.83e−02	−3.89e−02	1.00e+00	3.89e−02
−4.84e+00	1.00e+00	4.84e+00	−4.88e+00	1.00e+00	4.88e+00
−1.18e+1+3.06e+1i	3.59e−01	3.28e+01	−1.09e+1+3.06e+1i	3.36e−01	3.25e+01
−1.18e+1 − 3.06e+1i	3.59e−01	3.28e+01	−1.09e+1+3.06e+1i	3.36e−01	3.25e+01
−4.44e+01	1.00e+00	4.44e+01	−1.18e+1+3.06e+1i	3.59e−01	3.28e+01
−1.45e+02	1.00e+00	1.45e+02	−1.18e+1 +3.06e+1i	3.59e−01	3.28e+01
−6.14e+02	1.00e+00	6.14e+02	−4.48e+1	1.00e+00	4.48e+01
−7.96e+04	1.00e+00	7.96e+04	−1.47e+2	1.00e+00	1.47e+02
			−6.18e+2	1.00e+00	6.18e+02

Table 4
Participation factors of DFIG & DDPMSG based Wind-Diesel-Tidel hybrid system.

Participation factor Matrix (DFIG)

$$\begin{bmatrix} -0.01005 & -0.1057321 & -0.3401 & -0.998207 & -0.9982073 & 0.537238520 & -0.005066 & 0.352623952 \\ -2.821e-12 & -5.015e-07 & -2.9e-05 & 0.0013675 & 0.0013675 & 0.00052145 & -0.000868 & 0.259084091 \\ 4.9825019 & 0.00051230 & 0.00156 & 0.0011373 & 0.0011373 & -0.0028795 & -0.0561506 & 0.05316289 \\ 8.89e-08 & 0.98525017 & 0.70161 & -7.08e-05 & -7.082e-05-0.0079i & -0.398855 & 0.386126769 & -0.3104040 \\ -1.171e-05 & -0.02300 & 0.53168 & -0.00047 & -0.000472-0.00774i & -0.3693274 & 0.383014330 & -0.31038429 \\ 0.0104176 & 0.1066655 & 0.32580 & -0.003653 & -0.003653-0.0161i & -0.643635 & 0.837262837 & -0.695172 \\ -0.99989 & -0.078711 & -0.056 & -0.000553-0.00035i & -0.0005537+0.00034i & 0.03295079 & -0.002907 & -0.001607 \end{bmatrix} \begin{bmatrix} \Delta I_{dr}^{ref} \\ \Delta I_{dr} \\ \Delta V \\ \Delta E_{fd} \\ \Delta V_a \\ \Delta V_f \\ \Delta E_q^{'} \end{bmatrix}$$

Participation factor Matrix (DDPMSG)

$$\begin{bmatrix} \mathbf{-0.0000i} & \mathbf{-0.0000i} & \mathbf{0.0001-0.i} & \mathbf{-.4877+.162i} & \mathbf{-.4877-.162i} & \mathbf{-0.0049+0.0i} & \mathbf{-0.0004-0.0i} & 0 & 0 \\ \mathbf{-0.0000i} & \mathbf{0.0001+0.00i} & \mathbf{0.503-0.139i} & \mathbf{0.503+0.139i} & \mathbf{-0.0085-0.0i} & \mathbf{0.0001+0.0i} & \mathbf{0.0001+0.0i} & 0 & 0 \\ \mathbf{-0.0000i} & \mathbf{-0.0000i} & \mathbf{-0.0000-0.0i} & \mathbf{-.0122-.018i} & \mathbf{-.0122+.184i} & \mathbf{0.0002+0.0i} & \mathbf{-0.0033-0.0i} & 0 & 0 \\ \mathbf{-0.0000i} & \mathbf{.0001+0.0i} & \mathbf{-0.0074+0.0i} & \mathbf{-0.082+0.03i} & \mathbf{.0082-.003i} & \mathbf{0.0702+0.0i} & \mathbf{0.9452+0.0i} & 0 & 0 \\ \mathbf{-0.0000i} & \mathbf{0.9464+0.00i} & \mathbf{.1639--0.0i} & \mathbf{0.004-0.01i} & \mathbf{-.0012+0.06i} & \mathbf{-0.1109+0.0i} & \mathbf{-0.0003-0.0i} & 0 & 0 \\ \mathbf{-0.0000i} & \mathbf{0.032-0.0i} & \mathbf{1.3622-0.00i} & \mathbf{-0.0012-0.6i} & \mathbf{0.066+0.044i} & \mathbf{-0.3958+0.0i} & \mathbf{-0.0009-0.0i} & 0 & 0 \\ \mathbf{-0.0000i} & \mathbf{.0217+.0i} & \mathbf{-0.5199-0.0i} & \mathbf{0.066-0.044i} & \mathbf{-.0012+0.06i} & \mathbf{1.4506+0.0i} & \mathbf{0.0597-0.0i} & 0 & 0 \\ \mathbf{0.0000i} & \mathbf{1.0+0.00i} & \mathbf{-0.02+0.0i} & \mathbf{0.0010-0.0i} & \mathbf{-0.0000+0.0i} & \mathbf{-0.0000-0.0i} & \mathbf{-0.0008+0.0i} & 0 & 0 \\ 0 & 0 & 0 & 0 & 0 & 0 & 0 & \mathbf{-0.5+.1487i} & \mathbf{-0.5-0.1487i} \end{bmatrix} \begin{bmatrix} \Delta\omega_t \\ \Delta i_{ds} \\ \Delta i_{qs} \\ \Delta V_{dc} \\ \Delta V \\ \Delta E_{fd} \\ \Delta V_a \\ \Delta V_f \\ \Delta E_q^{'} \end{bmatrix}$$

the proposed hybrid system. The total region in right plane as covered by G (jω) indicates the Nyquist plot. If n indicates the number of poles which lie in the right-half of the s-plane, then there lie n map layers that leave behind the roots by traversing a small circle around each of them in anti-clockwise direction which results in a larger circle traversed in the clockwise direction that is clearly shown. The simulation results have shown that in comparison to the offshore hybrid system with DFIG, the DDPMG based hybrid system has better dynamic responses

4.2.2. Sensitivity analysis

Sensitivity analysis is carried out to see the robustness of the offshore wind-diesel-tidal hybrid system and optimum gains and parameters of the controller are obtained with different loading conditions. Sensitivity analysis identifies the parameters which have great impact on system stability. The sensitivity analysis results help in modelling those parameters as random variables during performing small signal stability analysis. As the power system is a nonlinear and complex system, the parametric sensitivity to the whole system matrix is very complex. Therefore the Sensitivity of few parameters which have direct entry to the system state matrix are computed analytically by studying their contribution to the state matrix. But for parameters having no direct entry to the state matrix sensitivity computation can be very complex.

5. Conclusion

Reactive power compensation and dynamic stability of isolated offshore wind tidal current hybrid system has been done and found to be effective. The small signal state space representation of the whole system has been done and a STATCOM is included as a device for reactive energy control. The offshore wind tidal hybrid turbines have been modelled with DFIG and DDPMSG and a comparison is drawn between the behaviour of different parameters. The simulation results vindicate the performance of DDPMSG based offshore wind tidal hybrid system which is further optimised with GA and PSO. In case of DDPMSG based hybrid system the oscillations of the terminal voltage damp quickly and the peak DC-link voltage is a little bit smaller than that of DFIG based hybrid system. During uncertainties or disturbances the DDPMSG turbines generate more reactive power to support the terminal voltage and improves the voltage stability profile of the hybrid system as it is interfaced with the power grid. The transient stability margins can be maximised by different soft computing based controllers through optimisation techniques like GA and PSO.

References

[1] M.L. Rahman, S. Oka, Y. Shiraj, IEEE Trans. Sustain. Energy 1 (2) (2010) 92–98.

[2] H.H. Hamed, M.E. El-Hawary, in: 24th annual Canadian IEEE Conference on Electrical and Computer Engineering, Niagara Falls Ontario, 2011.

[3] Mohammad Lutfur Rahman, Shunsuke Oka, Yasuyuki Shirai, Hybrid Offshore-wind and Tidal Turbine Power System for Complement the Fluctuation (HOTCF), Springer Academic Journals, 2010, pp. 177–186.

[4] Hamed H. Aly, El-Hawary, in: 23rd annual Canadian IEEE Conference on Electrical and Computer engineering, Calgary, Alberta, 2010 May 2–5.

[5] Hamed H.H. Aly, M.E. El-Hawary, Am. J. Energy Eng. 1 (1) (2013) 1–10.

[6] Mohammad Lutfur Rahman, Yasuyuki Shirai, Wind. Int. 6 (3) (2010) 28–31 May.

[7] Nishimura Kazuki. Study on Characteristics of Power Fluctuation Compensation in Hybrid Offshore-wind and Tidal Turbine Generation System. Master's thesis 2013; Kyoto University, February.

[8] Mohanty Asit, Viswavandya Meera, Prakash K. Ray, Patra Sandipan, Int. J. Electr. Power Energy Syst. 62 (2014) 753–762.

[9] Janaka B. Ekanayake, Holdsworth Lee, XueGuang Wu, Jenkins Nicholas, IEEE Trans. Power Syst. 18 (2) (2003) May 2–5.

[10] M.J. Khan, G. Bhuyan, A. Moshref, K. Morison, An Assessment of Variable Characteristics of the Pacific Northwest Regions Wave and Tidal Current Power Resources, and their Interaction with Electricity Demand & Implications for Large Scale Development Scenarios for the Region Tech. Rep, 17485-21-00, 2008 (Rep 3), Jan.

[11] Mihet-Popa Lucian, Blaabjerg Frede, Boldea Ion, IEEE Trans. Ind. Appl. 58 (1) (2004) January/February.

[12] Lei Yazhou, Mullane Alan, Lightbody Gordon, Yacamini Robert, IEEE Trans. Energy Convers. 28 (1) (2006) March.

[13] F. Wu, X.-P. Zhang, P. Ju, J. Electr. Power Eng. Res. 79 (2009) 650–655.

[14] Aly Hamed H. Forecasting, Modeling, and Control of Tidal currents Electrical Energy Systems. PhD thesis 2012; Halifax, Canada.

[15] Lutfur Rahman Mohammad, Shirai Yasuyuki, DC Connected Hybrid Offshore-wind and Tidal Turbine (HOTT) Generation System, Springer, Academic Journals, 2009, pp. 141–150.

[16] M.L. Rahman, S. Oka, Y. Shirai, Bangladesh Univ. Prof. J. 1 (2012) 2219–2251. ISBN: 2219–4851.

[17] M.L. Rahman, Y. Shirai, in: IEEE International Conference on Sustainable Energy Technologies (ICSET), 2008, pp. 650–655.

[18] Mohanty Asit, Viswavandya Meera, Mohanty Sthitapragyan, Aquat. Procedia 4 (2015) 1529–1536.

[19] Rahman M.L, Oka S., Shirai Y. Hybrid Wind-Tidal System Holds Potential to Guarantee Continuous Availability of Grid Power. Claremont Climate Report 2012, August 17.

[20] V.A. Marcus, J.A. Nunes, Peças Lopes, Hans Helmut, Ubiratan H. Bezerra, G. Rogério, IEEE Trans. Energy Convers. 28 (1) (2004) March.